SIMULATION X-RAY DIFFRACTION CURVES OF CeO_2 NANOPARTICLE BY USING DOUBLE VOIGT METHOD FOR CALCULATING THE CRYSTALLITE SIZE AND LATTICE STRAIN

Mustafa Mohammed Abdullah and Khalid Hellal Harbbi
mustafaaqq2@gmail.com
Department of Physics- College of Education (Ibn Al-Haitham) - University of Baghdad, Iraq

ABSTRACT : *In this study, the results of the Voigt method were used to simulate the x-ray diffraction of the cerium oxide nanoparticle to calculate the crystallite size and lattice strain obtained and then to compare the results obtained by this model with the results of the main method of the same powder using equations During which the calculation of the size of the crystallite size and lattice strain ,It was found that the results obtained from the new model were approximate to the original method where the values of the crystallite size (12.330917629nm) and the lattice strain (0.0057925108) of the new model respectively and the main method of Voigt were the results of the crystallite size (12.49640373 nm) and lattice strain (0.0068195988) respectively.*

Key words: double Voigt method, Voigt Function, Crystallite size, Lattice strain

INTRODUCTION

X-ray diffraction is the technique that found there first light by von Laue's researches in 1912, when he found that incident rays were diffracted by the crystals, therefor this tool was used to exploration the materials to find the perfect structure of the mater, at the beginning this technique was used for locating the structure of the crystals and in years later was highly developed for other uses and utilized in these days for various problems [1]. Diffraction Peak Profile Analysis (DPPA) it's a method that used to looking for the peaks and their shapes that fully developed by x-ray diffraction, it is useful technique for study the fine structure of the materials [2]. Normally the perspicuous crystal well spread to infinity, because of their limited size there is no perfect crystal, the broadened of diffraction peaks was made by this change from the pure crystal and two major features can be obtained from peak analysis they were the crystallite size and lattice strain, Crystallite size was the gauge of size of cohesively diffracted domain, due to the existence of polycrystalline assemblages the crystallite size is not the same as the particle size, lattice strain is gauge of the allocation of lattice constants that appears from the lattice defects [3]. The crystallite size and lattice strain were influenced the Bragg Peaks in various ways in which raise the width of the peaks also the intensity shifting the 2θ position, the strain change as tan θ change, and crystallite size change as 1/cos θ both of them effects on the peak broadening, size and strain both that caused by the broadening were intricate by take into account the width of the peak as function of 2θ [4]. One of the peak profile analysis methods was double Voigt method that described by Langford and derived the Voigt function and there equations for convolution the peaks, Cauchy and Gaussian profiles of the peaks can described by the 2w/β ratio from profile broadening [5].

Theory

Double Voigt method

Voigt function was used for fitting line profile this can be done by convolution the Lorentzian (L) function and the Gaussian (G) function [5]. Due to the broadening from the instrument in the experiment which is from the source that effect the line profile a correction must be taken in account h(x) is the experimental profile and f(x) is the sample profile and g(x) is the instrumental assistance

$$h(x) = f(x) * g(x) \quad (1)$$

Where (f,g,h) was Voigt function the f(x) can be found by:

$$\beta_{fL} = \beta_{hL} - \beta_{gL} \quad (2\ a)$$

$$\beta^2_{fG} = \beta^2_{hG} - \beta^2_{gG} \quad (2\ b)$$

Where β_{iL} was the Lorentzian component and β_{iG} was the Gaussian component and the β_i was the integral breadth which is [6]:

$$\beta = A / I_o \quad (3)$$

Where A was the area under the curve and the I_o was the highest intensity of the peak

$$\beta = K \lambda / \langle L \rangle \cos\theta \quad (4)$$

For the very small crystals the finite crystal size that can determine from the broadening showed by this equation where β was the breadth and K constant which is 0.89 used in this study and λ was the wavelength which is 0.15406 nm and θ was the Bragg angle and <L> was the average column length it was parallel to the diffracted planes which is the same as the circle length, there is a relation between the volume weighted column length and the volume weighted crystal diameter

$$\langle D \rangle = 4/3 \langle L \rangle \quad (5)$$

And the strain η from the broadening can be calculated from the equation

$$\beta = \eta \tan\theta \quad (6)$$

$$\beta \cos\theta = (K \lambda / \langle L \rangle) + \eta \sin\theta \quad (7)$$

The slope between the sin θ and β cos θ gives the strain η and the intercept gives the <L>

From the equations (4) and (6) the crystallite size and the strain can be estimated by changing the β to β_G and β_L for the Gaussian and Lorentzian profiles [7].

For h and g components the ratio 2w/β where 2w was the FWHM and β was the integral breadth for both the Gaussian (G) and the Lorentzian (L) profiles:

$$2w/\beta = 2/\pi = 0.63662 \quad \text{for Lorentz profile} \quad (8)$$

$$2w/\beta = 2*(\ln(2))^{1/2}/\pi^{1/2} = 0.93949 \quad \text{for Gaussian profile} \quad (9)$$

And by using the Williamson-Hall plot the crystallite size and lattice strain was calculated [8, 9].

Williamson-Hall method

The broadening in the lines caused by two factors the lattice strain and the crystallite size and also the instrumental broadening by assumption that the strain was uniform so that the Williamson-Hall equation that used for calculating the size and the strain

$$\beta_{h\,k\,l} = (K \lambda / D \cos\theta) + 4 \varepsilon \tan\theta \quad (10)$$

By multiply the equation by cos θ well be

$$\beta_{h\,k\,l} \cos\theta = (K \lambda / D) + 4 \varepsilon \sin\theta \quad (11)$$

Where $\beta_{h\ k\ l}$ was the integral breadth, θ was the Bragg angle, K was the shape factor which is constant (0.89), λ was the wavelength (0.15406 nm), D was the crystallite size and ε was the lattice strain, where the slop gives the strain and the intercept gives the crystallite size [10].

RESULTS AND DISCUSSIONS

New Model of Double Voigt Method

A new model of double Voigt method was developed by scaling plots of CeO_2 nanoparticles by using the standard peak of Silicon and CeO_2 peaks for correction purpose, the new plot was found by taking the deference between the h(x) which is the CeO_2 fitted peaks and the g(x) which is the standard peak, after that the integral breadth of the new peaks was estimated by the same was as original method by using eq. (3), which is showed in the figures and tables:

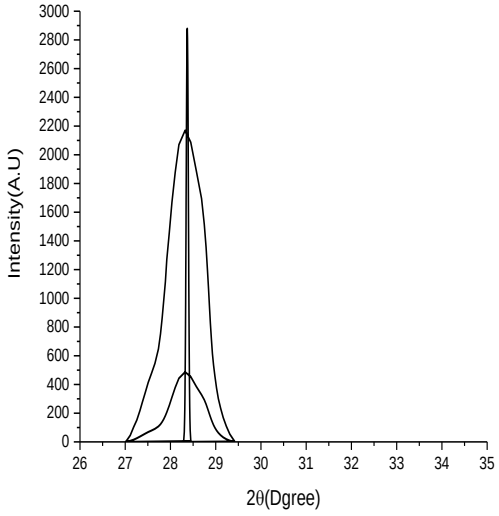

Figure (1)**new peak from standard peak - CeO_2 (111) peak.**

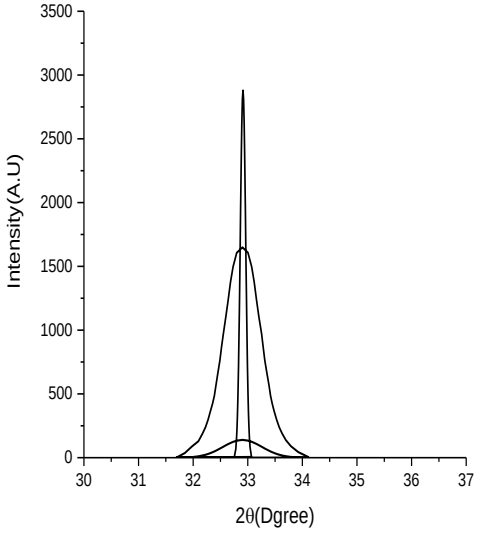

Figure (2)**new peak from standard peak - CeO_2 (200) peak.**

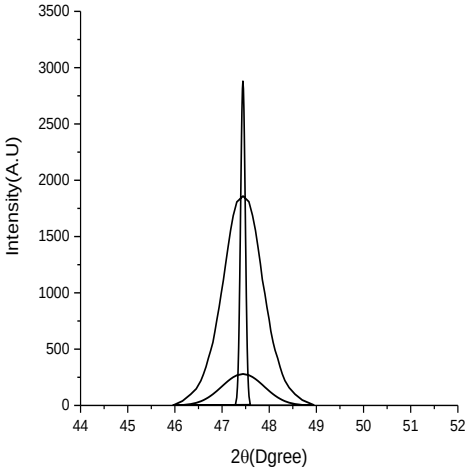

Figure (3) new peak from standard peak - CeO_2 (220) peak.

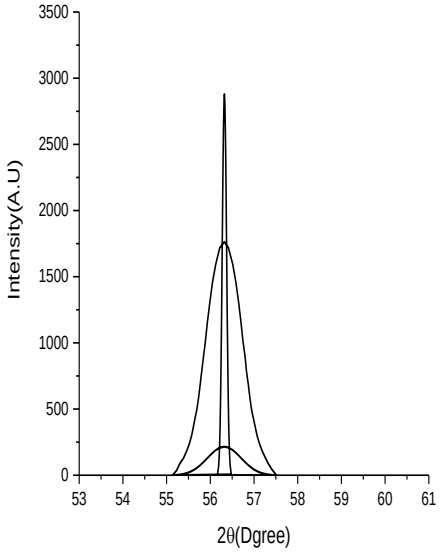

Figure (4) new peak from standard peak - CeO2 (311) peak.

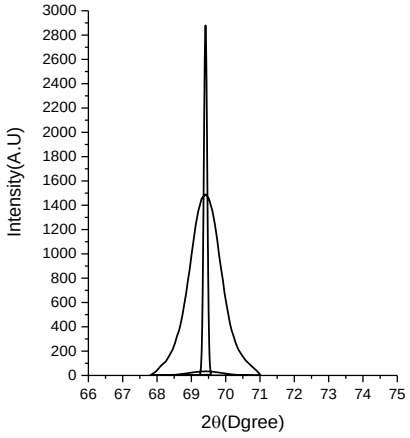

Figure (5) new peak from standard peak - CeO_2 (222) peak.

Table (1)results of the new peak from standard peak - CeO_2 (111) peak.

2θ (standard)	intensity (standard)	2θ (p111)	Intensity (p111)	2θ	intensity {median+ intensity(p111)}	Area under the curve	B= area/ Io
28.2907574	0	27.01076	0	27.01076	0	2.2623927388	1.0277821868
28.3055275	68.994497	27.11041	7.27302	27.11041	45.4067785	5.7661023346	
28.3129126	162.215995	27.18728	15.6716	27.18728	104.6153975	8.7485555218	
28.3162695	226.861775	27.25562	25.32268	27.25562	151.4149075	13.2090254953	
28.3202977	327.987405	27.32679	37.19189	27.32679	219.7815375	12.6891404812	
28.3229832	411.668805	27.37804	46.38002	27.37804	275.4044325	19.3099648356	
28.3256687	509.588505	27.44068	57.55943	27.44068	341.1333975	25.8144713294	
28.3283542	622.453645	27.50901	68.81476	27.50901	414.4489625	31.7421396374	
28.3303683	717.098495	27.58019	79.25697	27.58019	477.4347025	39.3552100013	
28.3323824	820.245735	27.65706	90.92294	27.65706	546.5072775	45.8800529666	
28.3350679	970.513255	27.73394	107.85724	27.73394	647.0424875	31.8579458052	
28.3377534	1134.182065	27.77949	123.11906	27.77949	751.7696225	29.8987168809	
28.3404388	1309.311245	27.8165	139.52329	27.8165	863.9405575	31.5731175016	
28.3431243	1493.216495	27.85067	158.30226	27.85067	984.0616375	38.8499574239	
28.3458098	1682.492395	27.88768	182.7483	27.88768	1115.3686475	37.357477317	
28.3491667	1920.408285	27.919	206.64144	27.919	1270.1663025	73.750013732	
28.3525235	2151.298745	27.9731	253.74491	27.9731	1456.2667375	93.4366646544	
28.3565518	2405.282955	28.03289	311.05767	28.03289	1669.2279825	126.1910494493	
28.36058	2618.072165	28.10406	378.61501	28.10406	1876.9585975	162.9603730812	
28.365951	2811.753105	28.18663	442.91347	28.18663	2070.2467575	289.7640445933	
28.37132	2879.503755	28.3233	486.89825	28.3233	2170.0992525	266.6264292962	
28.3766929	2811.968815	28.44857	453.82964	28.44857	2086.7288675	243.2829246887	
28.3820639	2618.474035	28.571	385.51415	28.571	1887.5082425	209.0507539975	
28.3860921	2405.790875	28.68773	327.58609	28.68773	1694.2745725	95.9454330248	
28.3901203	2151.877335	28.74752	292.80054	28.74752	1515.1394775	57.1749820094	
28.3934772	1921.017515	28.78738	262.09442	28.78738	1353.6503875	39.8753216361	
28.396834	1683.107655	28.8187	234.07508	28.8187	1192.6664475	25.7220526043	
28.3995195	1493.820665	28.84148	212.48306	28.84148	1065.6349225	20.0370525501	
28.402205	1309.892235	28.86141	193.44121	28.86141	945.1079325	17.6847174901	
28.4048905	1134.730015	28.88134	174.8068	28.88134	829.5752075	17.6120660529	
28.407576	971.020715	28.90411	154.57865	28.90411	717.3783325	15.1675276131	
28.4102615	820.707605	28.92689	135.94724	28.92689	614.2746625	14.7168364571	
28.4122756	717.524205	28.95251	117.21236	28.95251	534.5806425	14.1664186448	
28.4142897	622.842485	28.98099	99.22059	28.98099	460.2521275	15.451891601	
28.4169752	509.928415	29.018	79.86358	29.018	374.7595775	13.4617654352	
28.4196607	411.961415	29.05786	63.14138	29.05786	300.6927775	13.6876252687	
28.4223461	328.235575	29.10911	46.22711	29.10911	233.4584525	11.4477770355	
28.425703	242.024745	29.16605	31.75255	29.16605	168.6411975	9.4996130983	
28.4297312	162.362435	29.23438	18.81907	29.23438	109.4098225	6.2803112474	
28.4357736	81.898985	29.31126	8.68018	29.31126	53.9697625	3.0814398834	
28.449201	5.917311	29.41945	0.02338	29.41945	2.9937255		
						Σ = 2230.3893554153	

Table (2)results of the new peak from standard peak - CeO_2 (200) peak.

2θ (standard)	intensity (standard)	2θ (p200)	intensity(p200)	2θ	intensity {median+ intensity(p200)}	Area under the curve	B= area/ Io
32.7515148	0	31.69131	0.01888	31.69131	0.02832	2.8537477193	0.8680678161
32.781055	68.994497	31.84751	1.34273	31.84751	36.5113435	8.1338784371	
32.7958252	162.215995	31.97838	4.45691	31.97838	87.7933625	12.8218267381	
32.802539	226.861775	32.09659	10.47252	32.09659	129.1396675	12.1196897441	
32.8105954	327.987405	32.17258	17.23187	32.17258	189.8415075	11.8002863496	
32.8159664	411.668805	32.22746	22.90912	32.22746	240.1980825	12.5098938864	

32.8213374	509.588505	32.2739	29.17519	32.2739	298.5570375	14.0023440884	
32.8267084	622.453645	32.31611	35.78475	32.31611	364.9039475	14.956005705	
32.8307366	717.098495	32.35411	42.47	32.35411	422.2542475	15.2949623448	
32.8347648	820.245735	32.38788	48.96949	32.38788	483.5771025	15.5345704129	
32.8401358	970.513255	32.41743	55.05029	32.41743	567.8320625	20.7495475809	
32.8455068	1134.182065	32.45121	62.39181	32.45121	660.6787475	27.009138566	
32.8508776	1309.311245	32.4892	71.04895	32.4892	761.2290475	24.0065698924	
32.8562486	1493.216495	32.51875	77.9819	32.51875	863.5810975	30.9642584699	
32.8616196	1682.492395	32.55252	86.00334	32.55252	970.2512075	48.2020932375	
32.8683334	1920.408285	32.59896	96.95435	32.59896	1105.6356675	49.4200549354	
32.875047	2151.298745	32.64118	106.52543	32.64118	1235.4375175	55.1090583698	
32.8831036	2405.282955	32.68339	115.40397	32.68339	1375.7474325	66.6594336969	
32.89116	2618.072165	32.72983	123.99542	32.72983	1495.0292125	104.7430026422	
32.901902	2811.753105	32.79738	133.52895	32.79738	1606.1699775	171.7752573122	
32.91264	2879.503755	32.90292	139.49796	32.90292	1648.9988175	164.944048513	
32.9233858	2811.968815	33.00424	133.94655	33.00424	1606.9042325	104.7915904178	
32.9341278	2618.474035	33.07178	124.63726	33.07178	1496.1929075	66.7188346365	
32.9421842	2405.790875	33.11822	116.16432	33.11822	1377.1419175	55.1842232921	
32.9502406	2151.877335	33.16044	107.36435	33.16044	1236.9851925	49.4755733209	
32.9569544	1921.017515	33.20265	97.84296	33.20265	1107.2731975	52.6279500118	
32.963668	1683.107655	33.25331	85.91029	33.25331	970.4192625	27.121913142	
32.969039	1493.820665	33.28286	78.88859	33.28286	865.2432175	24.0633035156	
32.97441	1309.892235	33.31242	71.93979	33.31242	762.8558025	27.0696236797	
32.979781	1134.730015	33.35041	63.2475	33.35041	662.2362575	23.37376143	
32.985152	971.020715	33.38841	54.96757	33.38841	567.9617125	15.5381662785	
32.990523	820.707605	33.41796	48.89135	33.41796	483.6908275	13.4042524778	
32.9945512	717.524205	33.44751	43.18152	33.44751	423.5343825	13.3504919078	
32.9985794	622.842485	33.48128	37.14406	33.48128	367.1373325	15.4810026009	
33.0039504	509.928415	33.52772	29.73887	33.52772	299.5725125	12.5535045294	
33.0093214	411.961415	33.57416	23.3867	33.57416	241.0607575	11.8257429864	
33.0146922	328.235575	33.62904	17.19251	33.62904	189.9065525	11.0744692993	
33.021406	242.024745	33.69658	11.34611	33.69658	138.0315375	10.59491448	
33.0294624	162.362435	33.78946	5.95283	33.78946	90.1104625	9.0443947169	
33.0415472	81.898985	33.92455	1.89454	33.92455	43.7913025	4.5394209218	
33.068402	5.917311	34.11875	0	34.11875	2.9586555		
						Σ =1431.4428022871	

Table (3) results of the new peak from standard peak - CeO_2 (220) peak.

2θ (standard)	**intensity (standard)**	**2θ (p220)**	**intensity(p220)**	**2θ**	**intensity {median+ intensity(p220)}**	**Area under the curve**	**B= area/ Io**
47.0815148	0	45.96	0.162689	45.96	0.2440335	4.0320505793	1.0729671624
47.111055	68.994497	46.1611973	3.559521	46.1611973	39.83653	12.0271776976	
47.1258252	162.215995	46.3346432	11.827023	46.3346432	98.848532	14.5391030572	
47.132539	226.861775	46.4525865	22.843015	46.4525865	147.69541	17.8123906335	
47.1405954	327.987405	46.5497162	36.724169	46.5497162	219.079956	13.748776832	
47.1459664	411.668805	46.6052189	47.008638	46.6052189	276.3473595	17.2027341493	
47.1513374	509.588505	46.6607216	59.164386	46.6607216	343.5408315	18.4993008042	
47.1567084	622.453645	46.7092865	71.380441	46.7092865	418.297484	21.9617762414	
47.1607366	717.098495	46.7578514	85.055512	46.7578514	486.1325155	25.4097248802	
47.1647648	820.245735	46.8064162	100.113475	46.8064162	560.29308	25.321110499	
47.1701358	970.513255	46.8480432	114.014515	46.8480432	656.2784	29.4805940147	
47.1755068	1134.182065	46.8896703	128.696071	46.8896703	760.135139	39.6935356469	
47.1808776	1309.311245	46.9382351	146.58135	46.9382351	874.5276475	38.8092369174	

47.1862486	1493.216495	46.9798622	162.318743	46.9798622	990.086362	51.054751777	
47.1916196	1682.492395	47.028427	180.805907	47.028427	1112.455058	57.5778240813	
47.1983334	1920.408285	47.0769919	199.007395	47.0769919	1258.715235	64.5678206457	
47.205047	2151.298745	47.1255568	216.445177	47.1255568	1400.317138	82.0098348181	
47.2131036	2405.282955	47.1810595	234.804655	47.1810595	1554.84846	89.9165355943	
47.22116	2618.072165	47.2365622	250.795566	47.2365622	1685.2294315	133.2734854255	
47.231902	2811.753105	47.3128784	267.706449	47.3128784	1807.436226	241.6680641603	
47.24264	2879.503755	47.4446973	279.653193	47.4446973	1859.231667	229.0652201488	
47.2533858	2811.968815	47.5695784	268.877971	47.5695784	1809.301364	133.4526470918	
47.2641278	2618.474035	47.6458946	252.548348	47.6458946	1688.0595395	101.2497399284	
47.2721842	2405.790875	47.7083351	234.749408	47.7083351	1555.0195495	82.0200440124	
47.2802406	2151.877335	47.7638378	216.383508	47.7638378	1400.5139295	64.577615664	
47.2869544	1921.017515	47.8124027	198.942043	47.8124027	1258.921822	49.4430249704	
47.293668	1683.107655	47.8540297	183.367367	47.8540297	1116.604878	58.4691013004	
47.299039	1493.820665	47.9095324	162.251289	47.9095324	990.287266	38.8173913645	
47.30441	1309.892235	47.9511595	146.514941	47.9511595	874.718529	39.7024940799	
47.309781	1134.730015	47.9997243	128.632118	47.9997243	760.3131845	24.6353735231	
47.315152	971.020715	48.0344135	116.349854	48.0344135	660.0351385	29.6360784476	
47.320523	820.707605	48.0829784	100.056145	48.0829784	560.43802	21.8501609396	
47.3245512	717.524205	48.1246054	87.071346	48.1246054	489.3691215	25.192401194	
47.3285794	622.842485	48.1801081	71.333167	48.1801081	418.420993	18.5049012599	
47.3339504	509.928415	48.228673	59.122502	48.228673	343.6479605	15.1087468711	
47.3393214	411.961415	48.2772378	48.387411	48.2772378	278.561824	13.861801115	
47.3446922	328.235575	48.3327405	37.880302	48.3327405	220.9382405	17.0784840683	
47.351406	242.024745	48.4229324	24.509168	48.4229324	157.7761245	16.0741185223	
47.3594624	162.362435	48.5478135	12.315615	48.5478135	99.65464	11.2370110497	
47.3715472	81.898985	48.7004459	4.425779	48.7004459	47.588161	6.312342046	
47.398402	5.917311	48.9502081	0	48.9502081	2.9586555		
						Σ =1994.8945260522	

Table (4) results of the new peak from standard peak - CeO_2 (311) peak.

2θ (standard)	intensity (standard)	2θ (p311)	intensity(p311)	2θ	intensity {median+ intensity(p311)}	Area under the curve	B= area/ Io
56.1615148	0	55.13721	0.07067	55.13721	0.106005	1.7799420462	1.0141697814
56.191055	68.994497	55.23146	2.1116	55.23146	37.6646485	4.549486263	
56.2058252	162.215995	55.30371	4.77646	55.30371	88.2726875	8.821221129	
56.212539	226.861775	55.3854	9.50975	55.3854	127.6955125	12.9395746846	
56.2205954	327.987405	55.46708	16.7644	55.46708	189.1403025	12.1717288339	
56.2259664	411.668805	55.52363	23.668	55.52363	241.3364025	13.6510410704	
56.2313374	509.588505	55.5739	31.3188	55.5739	301.7724525	13.7022515767	
56.2367084	622.453645	55.61474	38.68124	55.61474	369.2486825	13.7622413664	
56.2407366	717.098495	55.6493	45.75205	55.6493	427.1773225	18.7859366702	
56.2447648	820.245735	55.69014	55.11808	55.69014	492.7999875	21.9800605351	
56.2501358	970.513255	55.73098	65.56136	55.73098	583.5986675	21.833032032	
56.2555068	1134.182065	55.76554	75.1973	55.76554	679.8869825	27.6010252245	
56.2608776	1309.311245	55.80324	86.46851	55.80324	784.3583875	34.3082192734	
56.2662486	1493.216495	55.84408	99.44109	55.84408	895.7698825	41.9598084965	
56.2716196	1682.492395	55.88806	114.07685	55.88806	1012.3614725	47.6351113902	
56.2783334	1920.408285	55.93204	129.10091	55.93204	1153.8555075	65.4408200122	
56.285047	2151.298745	55.98545	147.33551	55.98545	1296.6526375	86.4232920434	
56.2931036	2405.282955	56.04828	167.81723	56.04828	1454.3673225	114.883866734	
56.30116	2618.072165	56.12368	189.27601	56.12368	1592.9500975	150.8116497	

56.311902	2811.753105	56.21479	207.8089	56.21479	1717.5899025	185.9142144604	
56.32264	2879.503755	56.32161	215.69731	56.32161	1763.2978425	158.6656209185	
56.3333858	2811.968815	56.41271	209.36428	56.41271	1720.0308275	166.5842107325	
56.3441278	2618.474035	56.51325	189.68127	56.51325	1593.7589225	110.2024642256	
56.3521842	2405.790875	56.5855	169.28859	56.5855	1456.8283225	90.873663479	
56.3602406	2151.877335	56.65148	147.87674	56.65148	1297.7537775	61.6903143447	
56.3669544	1921.017515	56.70175	130.731	56.70175	1156.6052575	47.7554203295	
56.373668	1683.107655	56.74573	115.68598	56.74573	1015.0827975	48.0084721214	
56.379039	1493.820665	56.79599	98.9411	56.79599	895.3219825	26.4500579228	
56.38441	1309.892235	56.82741	88.91772	56.82741	788.3226975	32.3072823835	
56.389781	1134.730015	56.87139	75.66196	56.87139	680.8579475	21.8653932384	
56.395152	971.020715	56.90595	65.9934	56.90595	584.5004575	20.344248548	
56.400523	820.707605	56.94365	56.27748	56.94365	494.7700225	20.2897700333	
56.4045512	717.524205	56.98763	46.0997	56.98763	427.9116525	15.0217646215	
56.4085794	622.842485	57.02533	38.38513	57.02533	368.9989375	14.7317480843	
56.4139504	509.928415	57.06932	30.54266	57.06932	300.7781975	14.43871546	
56.4193214	411.961415	57.12273	22.61047	57.12273	239.8964125	12.7569203872	
56.4246922	328.235575	57.18242	15.61661	57.18242	187.5427025	11.6559097075	
56.431406	242.024745	57.25467	9.39991	57.25467	135.1122375	7.7496262272	
56.4394624	162.362435	57.32379	5.29561	57.32379	89.1246325	5.6479377547	
56.4515472	81.898985	57.40861	2.06703	57.40861	44.0500375	2.2893233491	
56.478402	5.917311	57.50601	0	57.50601	2.9586555		
						Σ =1788.2833874109	

Table (5) results of the new peak from standard peak - CeO_2 (222) peak.

2θ (standard)	intensity (standard)	2θ (p222)	intensity(p222)	2θ	intensity {median+ intensity(p222)}	Area under the curve	B= area/ Io
69.2515148	0	67.8018922	0	67.8018922	0	3.0381468877	1.1833530231
69.281055	68.994497	67.9759961	0.2687601	67.9759961	34.90038865	8.5930711086	
69.2958252	162.215995	68.1226099	0.8080726	68.1226099	82.3201064	13.6385539746	
69.302539	226.861775	68.2600604	1.7996101	68.2600604	116.13030265	15.6580109095	
69.3105954	327.987405	68.3700207	3.113258	68.3700207	168.6635895	15.7206717628	
69.3159664	411.668805	68.452491	4.4976335	68.452491	212.58085275	16.3672044103	
69.3213374	509.588505	68.5212162	5.9557119	68.5212162	263.72782035	17.4559602715	
69.3267084	622.453645	68.5807781	7.4603575	68.5807781	322.41735875	22.2889280246	
69.3307366	717.098495	68.6449216	9.3360932	68.6449216	372.5533873	18.3021381379	
69.3347648	820.245735	68.6907384	10.8337967	68.6907384	426.37356255	25.5882726197	
69.3401358	970.513255	68.7457186	12.7916967	68.7457186	504.44417255	27.5583221042	
69.3455068	1134.182065	68.7961171	14.7210357	68.7961171	589.17258605	34.8915280666	
69.3508776	1309.311245	68.8510973	16.9410377	68.8510973	680.06717905	33.3306696018	
69.3562486	1493.216495	68.8969141	18.8524227	68.8969141	774.88688155	45.3007867827	
69.3616196	1682.492395	68.9518943	21.1743337	68.9518943	873.00769805	51.3629788476	
69.3683334	1920.408285	69.0068745	23.4703167	69.0068745	995.40961755	62.8328559735	
69.375047	2151.298745	69.0664363	25.8522587	69.0664363	1114.42776055	75.6691034333	
69.3831036	2405.282955	69.1305799	28.1976117	69.1305799	1244.93789505	95.2869617103	
69.39116	2618.072165	69.2038868	30.4656037	69.2038868	1354.73448805	135.1552995424	
69.401902	2811.753105	69.3001021	32.5490827	69.3001021	1454.70017655	161.8938431655	
69.41264	2879.503755	69.4100625	33.4216117	69.4100625	1489.88429505	148.4195762275	
69.4233858	2811.968815	69.5108595	32.7012037	69.5108595	1455.03621305	141.6298385734	
69.4341278	2618.474035	69.6116565	30.6175007	69.6116565	1355.16326855	95.3225081712	
69.4421842	2405.790875	69.6849634	28.3889837	69.6849634	1245.47891305	81.1045465913	
69.4502406	2151.877335	69.7536886	25.8925467	69.7536886	1114.77748755	53.1986171768	

69.4569544	1921.017515	69.8040871	23.8885487	69.8040871	996.34158055	59.9652883879	
69.463668	1683.107655	69.8682306	21.2183897	69.8682306	873.38141205	45.3211776331	
69.469039	1493.820665	69.9232108	18.8963917	69.9232108	775.25492005	30.0183517896	
69.47441	1309.892235	69.9644459	17.1734077	69.9644459	680.70622905	34.9257920159	
69.479781	1134.730015	70.0194261	14.9432927	70.0194261	589.77994655	30.0889037115	
69.485152	971.020715	70.0744063	12.8304547	70.0744063	504.75603955	23.4768662085	
69.490523	820.707605	70.1248048	11.0263737	70.1248048	426.89336305	18.3250036855	
69.4945512	717.524205	70.1706216	9.5130758	70.1706216	373.0317162	20.7294691949	
69.4985794	622.842485	70.2301835	7.741187	70.2301835	323.033023	18.8302671853	
69.5039504	509.928415	70.294327	6.0881099	70.294327	264.09637235	18.5656278947	
69.5093214	411.961415	70.3722156	4.4303458	70.3722156	212.6262262	18.3313245316	
69.5146922	328.235575	70.4684309	2.8693341	70.4684309	168.42178865	16.7136199961	
69.521406	242.024745	70.582973	1.5996643	70.582973	123.41186895	15.5391495508	
69.5294624	162.362435	70.7341685	0.6382249	70.7341685	82.13855485	9.8887712721	
69.5415472	81.898985	70.8945273	0.1633461	70.8945273	41.19451165	2.7310774482	
69.568402	5.917311	71.0182327	0.0009145	71.0182327	2.96002725	Σ =1763.0590845809	

After calculate the integral breadth of the new model, the crystallite size <D> and the apparent strain η of the new model was estimated by using the same equations of the original double Voigt method by using the eq. (5) and the eq. (7) the results were in the tables:

Table (6) results of new model used to calculate crystallite size and apparent strain.

2θ	θ	B_G	B_L	Sin θ	Cos θ	B_L Cos θ	B_G Cos θ	Tan θ
28.3233	14.16165	1.0277821868	1.2881339449	0.2446584485	0.9696093252	1.2489866851	0.9965471927	0.2523268311
32.90292	16.45146	0.8680678161	1.0879616661	0.2832029473	0.9590600037	1.0434205195	0.8325291229	0.2952922092
47.4446973	23.72234865	1.0729671624	1.3447649136	0.4023049072	0.9155057409	1.2311399986	0.982307597	0.4394346088
56.32161	28.160805	1.0141697814	1.2710733246	0.4719477707	0.8816265092	1.1206119381	0.8941189641	0.5353148593
69.4100625	34.70503125	1.1833530231	1.4831130733	0.5693517152	0.8220940484	1.2192584306	0.9728274774	0.6925627504

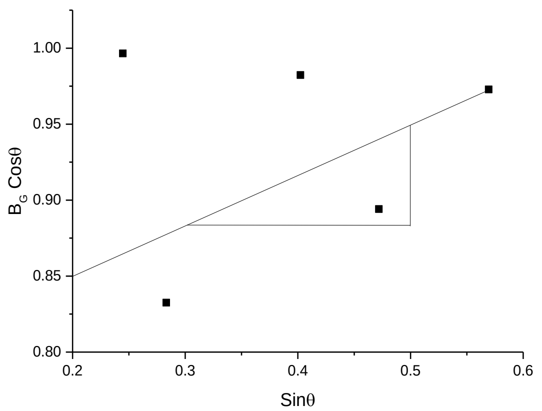

Figure (6) new model plot of relation between B G Cos θ and Sin θ.

Table (7) results of the crystallite size in (nm) and apparent strain of the new model.

1	2	the intercept	<L>vol= K λ / the cut	<D>= 4/3 <L>vol	The Slope (η)
X = 0.301102703; Y = 0.883452869	X = 0.499762162; Y = 0.949385246	0.849465749	9.2481882218	12.330917629	0.0057925108

The separation double Voigt method also used to estimate the crystallite size<D> in the (nm) and the apparent strain η for the new model by the eq. (4) and eq. (5) and eq. (6) and the results for this method were in the table below:

Table (8) results of new model by using separation double Voigt method

K	λ	<L>vol= K λ / B Cos θ	<D>= 4/3 <L>vol	η = B / tanθ
0.89	0.15406 nm			
		6.2899142388	8.3865523184	0.071091065
		7.5291016307	10.0388021742	0.0513072849
		6.38109325	8.5081243334	0.0426156916
		7.0104724636	9.3472966182	0.0330657772
		6.4432764521	8.5910352695	0.0298217114
		Average =6.7307716071	Average =8.9743621427	Average =0.045580306

CONCLUSION

By using the Double Voigt method a high accuracy results can be obtained of the crystallite size and lattice strain compared with other method that used for analysis the peak broadening profile, it was found that there is a need to develop the method used in the study to compare the results with the original method. This method was developed by scaling plot for the diffraction lines of the desired model to measure its crystallite size, the lattice strain obtained and the standard model. The results were very close to both crystallite size and lattice strain in case of separation and scaling plots.

REFERENCES

[1] B. D. CULLITY, ELEMENTS OF X-RAY DIFFRACTION,Notre Dame, Indiana: ADD1SON-WESLEY, 1956, p. 1.

[2] Simm, Thomas, "THE USE OF DIFFRACTION PEAK PROFILE ANALYSIS IN STUDYING THE PLASTIC DEFORMATION OF METALS," School of Materials, University of Manchester, Manchester, 2012.

[3] P. Bindu,Sabu Thomas, "Estimation of lattice strain in ZnO nanoparticles: X-ray peak," J Theor Appl Phys, vol. 8, no. 4, p. 123–134, 2014.

[4] Y. T. Prabhu, K. Venkateswara Rao, V. Sesha Sai Kumar, B. Siva Kumari, "X-ray Analysis of Fe doped ZnO Nanoparticles by Williamson-Hall and Size-Strain Plot," International Journal of Engineering and Advanced Technology (IJEAT), vol. 2, no. 4, pp. 268-274, 2013.

[5] J. I. Langford, "A Rapid Method for Analysing the Breadths of Diffraction and Spectral Lines using the Voigt," J. Appl. Cryst, vol. 11, no. 1, pp. 10-14, 1978.

[6] J. I. Langford, "The Use of the Voigt Function in Determining Microstructural Properties from," in Accuracy in Powder Diffraction II, Gaithersburg, 1992.

[7] Meier, Mike L., "MEASURING CRYSTALLITE SIZE USING X-RAY DIFFRACTION,THE WILLIAMSON-HALL METHOD," University of California, Davis, California, 2005.

[8] H. G. Jiang, M. Rühle and E. J. Lavernia, "On the applicability of the x-ray diffraction line profile analysis in extracting grain size and microstrain in nanocrystalline materials," Journal of Materials Research, vol. 14, no. 2, pp. 549-559, 1999.

[9] Xiaolu Pang, Kewei Gao, Fei Luo, Yusuf Emirov, Alexandr A. Levin, Alex A. Volinsky, "Investigation of microstructure and mechanical properties of multi-layer Cr/Cr2O3 coatings," Thin Solid Films, vol. 517, no. 6, pp. 1922-1927, 2009.

[10] Sadia Perveen, Muhammad Akhyar Farrukh, "Influence of lanthanum precursors on the heterogeneous La/SnO2–TiO2 nanocatalyst with enhanced catalytic activity under visible light," Journal of Materials Science: Materials in Electronics, vol. 28, no. 15, p. 10806–10818, 2017.